EPJ Web of Conferences **57**, 03003 (2013)
DOI: 10.1051/epjconf/20135703003

A quasi-continuous superradiant Raman laser with < 1 intracavity photon

Justin G. Bohnet[1], Zilong Chen[1], Joshua M. Weiner[1], Kevin C. Cox[1], Dominic Meiser[2], Murray J. Holland[1] and James K. Thompson[1,a]

[1] *JILA, University of Colorado and NIST, and Dept. of Physics, University of Colorado, Boulder, Colorado 80309, USA*
[2] *Current Affiliation: Tech-X Corp., 5621 Arapahoe Ave. Ste. A, Boulder, Colorado 80303, USA*

Abstract. Steady-state collective emission from ensembles of laser cooled atoms has been proposed as a method for generating sub-millihertz linewidth optical lasers, with potential for broad impacts across science and technology. We have built a model system that tests key predictions for such active oscillators using a Raman laser with laser cooled atoms as the gain medium. The laser operates deep in the bad-cavity, or superradiant, regime of laser physics, where the cavity decay rate is much greater than the atomic coherence decay rate. Specifically, we demonstrate that a system of 10^6 ^{87}Rb atoms trapped in a 1D standing wave optical lattice can spontaneously synchronize and collectively emit a quasi-continuous coherent optical output, even when the intracavity field contains on average < 1 photon.

1. INTRODUCTION

Collective effects in cold atom systems are being pursued for advancing precision measurements beyond limits imposed by single-atom physics [1–6]. Recent proposals suggest using collective emission, or superradiance, to enhance the radiation rates of ultranarrow linewidth transitions in alkaline-earth elements to realize millihertz linewidth optical frequency standards [7–10]. The superradiant enhancement results from spontaneous synchronization of the individual atomic radiating dipoles as a result of cavity-mediated interactions between the dipoles. Superradiant light sources are optical realizations of an extreme bad-cavity laser [11, 12] similar to active masers [13].

To study the physics of these proposed superradiant laser systems, we have constructed a superradiant Raman laser that uses $\sim 10^6$ laser cooled ^{87}Rb atoms trapped in a 1D optical lattice as the gain medium [14]. The lasing utilizes an effective optical decay between the metastable ground clock states separated by 6.8 GHz. The variable rate decay is induced using an optical Raman transition through an intermediate excited state. While this "physics test-bed" does not have the precision of a true narrow optical transition as exists in alkaline-earth atoms, the tunable decay rate provides a degree of freedom to scale the relevant rates in the system in order to explore the physics and test predictions for future implementations of optical active oscillators.

In this article, we provide an overview of our work with this superradiant Raman laser. Details for the work described here can be found in Refs. [14–17]. First, in Sec. 2, we describe how superradiant lasers differ from the more typical good-cavity optical laser. Then in Sec. 3, we describe our superradiant Raman laser and how it models proposed superradiant light sources. In Sec. 4, we show the

[a]e-mail: jkt@jila.colorado.edu

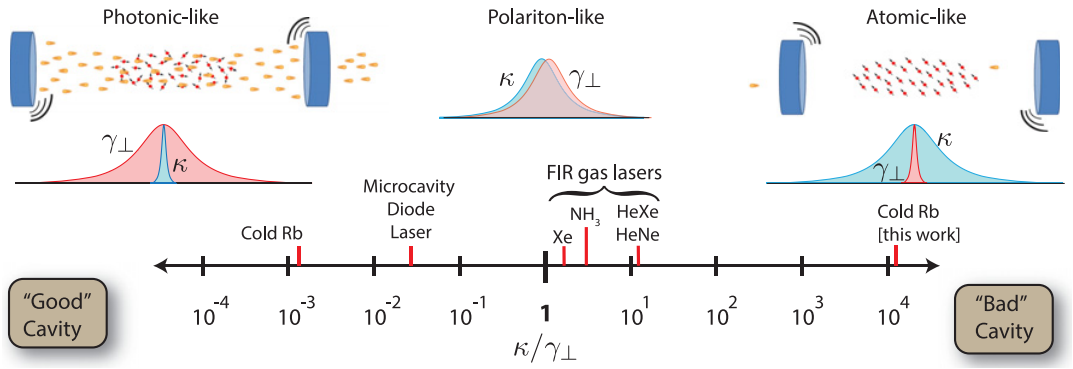

Figure 1. In the good-cavity limit, the atomic coherence rapidly decays, and the photon field is the primary reservoir of phase information in the laser. As a result, perturbations which disturb the cavity resonance frequency, such as thermal mirror vibrations (drawn as curved lines near the mirrors), limit the frequency stability of the laser. At the other extreme, the bad-cavity, or superradiant, laser presented here operates in a regime where the atomic coherence decay rate $\gamma_\perp$ is much less than the cavity power decay rate κ. In this regime, the atomic gain medium is the primary reservoir of phase memory in the laser, a fact represented by the aligned dipoles of the atoms and a cavity mode nearly devoid of light quanta. Because the emission frequency is primarily determined by the atoms, perturbations from fluctuations in the cavity frequency are suppressed. Near the crossover regime, the phase coherence is jointly stored by the atoms and the cavity photons, making it a polariton-like excitation. Most optical lasers operate in the good-cavity limit (one example is the cold atom Raman laser of Ref. [19]), with microcavity diode lasers [20] and far infrared (FIR) gas lasers, using Xe [21], NH_3 [22, 23], and HeXe/HeNe [12], operating in the vicinity of the crossover, polariton-like regime. Our cold atom Raman laser is unique both in terms of operating so deeply into the bad-cavity regime, and also in that the steady-state intracavity photon number can be made much less than one.

quasi-continuous operation of our superradiant laser which nondestructively maps the robust coherence of the atomic system onto the cavity light field, and we discuss the limitation to the lasing duration imposed by atom loss in the system. Next, in Sec. 5, we discuss the behavior of the system as a function of the incoherent repumping rate, which is necessary for steady-state operation in order to recycle the atoms after photon emission. However, the repumping also causes decoherence on the lasing transition, eventually leading to a quenching of the laser oscillation as the repumping rate is increased. Finally, in Sec. 6, we confirm that the superradiant laser has a greatly reduced sensitivity to the cavity resonance frequency. It is this insensitivity to the cavity that may make the proposed optical frequency references highly immune to both thermal and technical cavity vibrations, offering the potential for such sources to operate outside of carefully controlled laboratory environments [18].

2. LASER REGIME COMPARISON

To understand some of the non-intuitive properties of superradiant lasers, it is useful to consider the relationship between the good-cavity and bad-cavity regime. We use the terms "bad-cavity" and "superradiant" synonymously to refer to the laser regime defined using the ratio between the laser cavity power decay rate κ and the gain bandwidth or atomic coherence decay rate $\gamma_\perp$. Here $\gamma_\perp$ includes contributions from the natural linewidth, as well as other broadening mechanisms, such as inhomogeneous transition frequencies across the sample and the necessary homogeneous broadening from the repumping lasers. Most optical lasers operate in the good-cavity regime $\kappa/\gamma_\perp \ll 1$(see left side Fig. 1). In the opposite regime to our work, a laser-cooled ^{87}Rb Raman laser was recently demonstrated to operate deep in the good-cavity regime in Ref. [19].

In the good-cavity regime, the phase coherence is primarily stored in the cavity light field, and the polarization of the gain medium adiabatically follows the state of the cavity field. As a result, the laser

frequency and linewidth is determined primarily by the cavity properties, with the familiar quantum-limited linewidth given by the Schawlow-Townes limit [24] as $\Delta f_{GC} \propto \frac{\kappa}{M_c}$ where M_c is the average number of intracavity photons. The Schawlow-Townes limit can be made quite small in optical lasers, and the linewidth is instead limited by the laser cavity frequency stability or the stability of an external optical reference. In particular, the fundamental stability of state of the art optical cavitites is limited by thermal mirror noise [25]. Superradiant optical lasers may provide a means to circumvent this issue.

Deep in the superradiant limit, the roles of the atoms and photons have been reversed in some ways. Here the cavity field rapidly decays, and the phase coherence resides primarily in the atom's robust collective coherence. In fact, such lasers were predicted to operate with a very small intracavity field – just enough to maintain the synchronization between the individual atomic dipoles. This means that the laser frequency properties are determined largely by the atoms (right side of Fig. 1). In this limit, the Schawlow-Townes linewidth is set by atomic properties $\Delta f_{BC} \propto \frac{\gamma_\perp}{N}$, analogous to the good-cavity case, but with the number of atomic quanta N replacing the photonic quanta M_c and the cavity damping rate κ replaced by the atomic decoherence rate $\gamma_\perp$. Additionally, the laser frequency is mainly determined by the atomic transition frequency, with the sensitivity to cavity frequency changes being reduced by the ratio $\gamma_\perp/\kappa$. The roles of the light field and atoms are not completely reversed though. Energy is still supplied to the system by optically pumping the atoms, a fact that will lead to a laser quenching threshold discussed below.

Active maser oscillators have operated deep into the superradiant regime at microwave frequencies [13]. Attempts to operate optical lasers in the bad-cavity regime have mainly been confined to far infrared (FIR) gas lasers operating much closer to the crossover regime $\kappa = \gamma_\perp$ [12, 21–23] in which the excitation of the oscillator is described best as a polariton, possessing significant atomic and photonic contributions (Fig. 1 center). Semiconductor microcavity lasers have very high cavity decay rates due to their small size, and have also attempted to enter the bad-cavity regime for the benefits of low threshold lasing, but have to the best of our knowledge, not realized $\kappa/\gamma_\perp > 1$ [20]. Previous related experiments with cold-atom Raman lasers also operated in the superradiant limit [26–28], but did not study the spectral properties of the light in detail and operated with large intracavity photon numbers $M_c \gg 1$.

3. A PHYSICS "TEST-BED" FOR STEADY-STATE SUPERRADIANCE

To test the physics of proposed superradiant light sources, we have realized a cold-atom Raman laser that operates deep into the superradiant regime with $\kappa/\gamma_\perp > 10^4$ [14]. The laser uses $N = 10^6$ ^{87}Rb atoms at $\approx 40\,\mu$K confined in a 1D standing wave optical lattice formed in the optical cavity. The cavity has a power decay rate $\kappa/2\pi = 11.1$ MHz. As shown in Fig. 2, the Raman laser emulates the narrow linewidth transition of alkaline-earth elements using the metastable ground states of ^{87}Rb. We create an effective optical decay with a dressing laser (with Rabi frequency Ω_d) detuned by Δ from an optically excited intermediate state $|i\rangle$ with linewidth Γ. The effective two-level system (see Ref. [29] for details) has an effective excited state decay rate $\gamma_{eg} = \Gamma\frac{\Omega_d^2}{4\Delta^2}$ that can be controlled with the intensity of the dressing laser. We typically operate with γ_{eg} ranging from 2 to 60 s^{-1}.

The phase noise of the dressing laser is also imposed on the emitted light's phase, making this source technologically uninteresting as a stable optical phase reference. However, the tunability of the decay rate γ_{eg} has proven helpful for exploring the physics of these light sources. The emitted light is detected in heterodyne with the dressing laser, removing the dressing laser's phase noise for our studies.

The effective single particle cooperativity, $C = \frac{(2g_2)^2}{\kappa\gamma_{eg}}$, gives the ratio with which the atom decays from $|e\rangle$ to $|g\rangle$ by emitting a photon into the cavity mode compared to all other free space modes, and is equivalent to the Purcell factor [30]. Here g_2 is the two-photon coupling of the atoms to the cavity mode after adiabatic elimination of the intermediate state [29]. The laser operates in the single particle weak coupling limit $C = 8 \times 10^{-3} \ll 1$ such that a single atom scarcely experiences the presence of the cavity. However, the collective coupling $NC \approx 10^4 \gg 1$ is strong, a key requirement for the

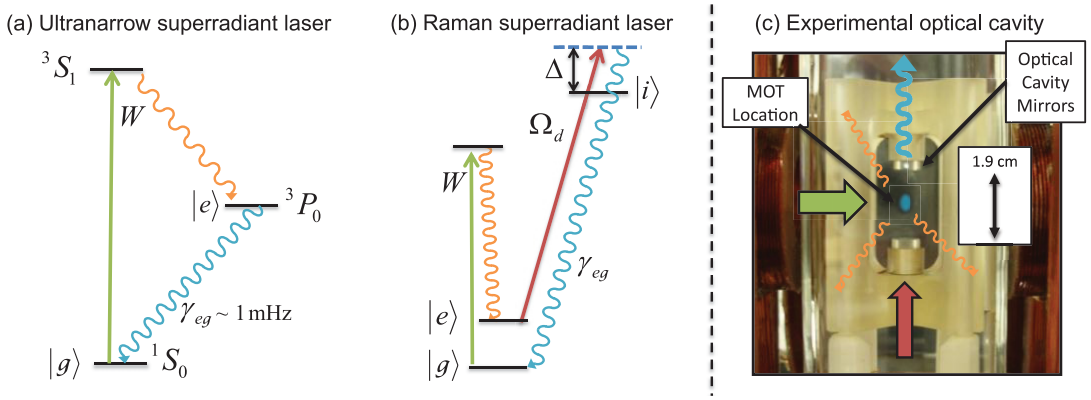

Figure 2. Simplified energy level diagrams of (a) a proposed superradiant light source using an ultra-narrow optical transition in alkaline-earth atoms (Sr, Yb, Ca, etc.) and (b) a superradiant Raman laser. Proposed superradiant lasers collectively enhance the emission rate of the nearly-forbidden optical transition $|e\rangle$ to $|g\rangle$ with single particle excited state decay rate γ_{eg}. Non-collective repumping of $|g\rangle$ back to $|e\rangle$ at rate W recycles the atoms to the excited state after they emit a photon. The superradiant Raman laser uses an effective optical transition, induced by a dressing laser with Rabi frequency Ω_d, to create a tunable excited state decay rate γ_{eg}. The dressing laser is detuned from an intermediate optically excited state $|i\rangle$ by Δ. (c) The optical cavity used in our realization of a superradiant Raman laser. The separation between the cavity mirrors is 1.9 cm. We load atoms into the standing wave optical lattice trap from a MOT formed between the mirrors (false color). The dressing laser (red) is applied non-resonantly along the cavity axis. The repumping light (green) is applied perpendicular to the cavity axis. The emitted light (blue) is detected in upper port, though it is emitted into the lower cavity output port as well (not shown). The single-particle repumping light is scattered into free space (orange).

atoms to collectively establish a strong superradiant coupling to the cavity mode, providing a collective enhancement with direct analogy to a classical phased-array antenna [31].

4. STEADY-STATE SUPERRADIANCE

The spontaneous synchronization of the individual atomic dipoles leads us to represent the collective state of the atoms at the heart of the superradiant laser with a Bloch vector $\vec{J}$ [32]. The vector's axial projection $J_z = \frac{1}{2}\langle\sum_{q=1}^{N} |e\rangle^{(q)}\langle e|^{(q)} - |g\rangle^{(q)}\langle g|^{(q)}\rangle$ is proportional to the laser inversion. The magnitude of the vector's projection onto the equatorial plane $J_\perp = |\langle\sum_{q=1}^{N} |g\rangle^{(q)}\langle e|^{(q)}\rangle|$ is related to the average degree of coherence between $|e\rangle$ and $|g\rangle$, or equivalently the atomic polarization. Here the sums run over individual atoms, indexed by q.

In the superradiant regime, the azimuthal angle of the Bloch vector ϕ evolves on average at a frequency very close to the atomic transition frequency. The fundamental Schawlow-Townes stability of the system is limited by phase diffusion of the Bloch vector driven by quantum noise [7, 9, 10]. Due to its rapid decay, the cavity field in a superradiant laser is largely slaved to follow the collective atomic dipole. We graphically represent this as a mapping of the 3D Bloch vector onto a 2D phasor representing the cavity field, shown in Fig. 3(a). The light phase Ψ adiabatically follows the atomic phase ϕ and the light field amplitude A follows the projection $J_\perp$.

Superradiant emission in the optical domain is often thought of as a pulsed phenomenon [31, 33]. However, proposed superradiant light sources [7, 8] are predicted to operate continuously by incoherently recycling or repumping atoms from the ground state back to the excited state. The continuously emitted light field then acts as a continuous non-destructive readout of the collective atomic phase. In Fig. 3(b) we show the laser amplitude A and phase Ψ when the laser is operating quasi-continuously. Even with an average output amplitude corresponding to ~ 3 intracavity photons,

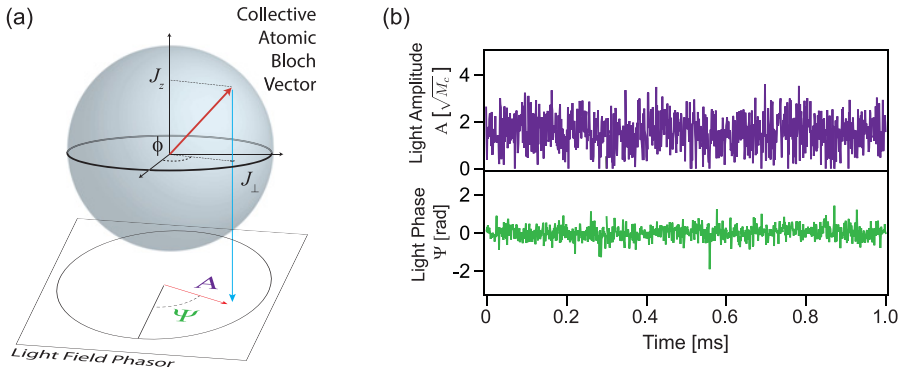

Figure 3. (a) In steady-state, the individual atomic dipoles in a superradiant laser have spontaneously synchronized. We represent their state with a collective atomic Bloch vector (red) and assume we are in a frame co-rotating with the vector, so the collective atomic azimuthal phase ϕ is constant, up to phase diffusion set by quantum noise. Operating deep into the bad-cavity regime of laser physics, the cavity field in the superradiant laser is essentially slaved to the atomic coherence. We represent this as a direct mapping from the Bloch vector to the cavity field phasor with amplitude A and phase Ψ. Thus, the phase stability of the output light field is due to the stability of the evolution of ϕ. (b) The result is that even for an output light field amplitude A that corresponds to an average of ~ 3 intracavity photons, the light phase Ψ is stable and well defined.

the phase remains well defined. As detailed in Ref. [16], we find that the optimal estimation of the underlying atomic phase ϕ using the measured light phase corresponds to an exponentially weighted average of the light phase measured at previous times. The precision of the mapping can in principle be near the standard quantum limit for a coherent state of the N atom ensemble and is forgiving of finite detection efficiency.

We can dynamically control the phase mapping of the atomic coherence onto the light field through control of the dressing laser intensity. Because the atoms are the reservoir of phase information, the laser's phase can be preserved even when the laser is not emitting light–a condition achieved by quickly switching off the dressing and repumping lasers. The dynamic control of the laser emission presents the unique opportunity to realize a hybrid active/passive atomic sensor. In Ref. [16], we proposed such a sensor and demonstrated its operation in our ^{87}Rb system. In Ref. [17], we demonstrated a superradiant Raman magnetometer that exploited dynamic control of the lasing to switch between active broad band sensing, and passive Ramsey-like measurements for narrow-band lock-in detection of fields.

By decreasing the intensity of the dressing laser, we could smoothly lower γ_{eg}, also lowering the steady-state intracavity photon number. We were able to show that even with an output power that corresponded to 0.2 intracavity photons on average, we could see a phase coherent output beam with a 350 Hz linewidth, a factor of 3×10^3 below the repumping-induced broadening of the bare transition [14]. We were not able to observe the predicted quantum noise limited linewidth, likely due to technical noise associated with losing atoms from the trap.

The time for which our laser oscillates far exceeds the length of pulsed superradiant emission, which usually lasts 1–2 μs in our experiment. Figure 4(a) shows the emitted power approaching zero after lasing for ~ 10 ms. By varying the excited state lifetime and repumping rates, we were also able to observe superradiant emission lasting as long as 120 ms. In Ref. [14] we stated that the turn off was due to losing atoms from the optical lattice trap. Here we present data that supports this conclusion. We measure the atom loss by starting superradiant emission and after a variable emission time, switching off the dressing and repumping laser, which stops the emission and freezes the population. Immediately afterwards, we probe the resonant frequency of the cavity, which is dispersively shifted

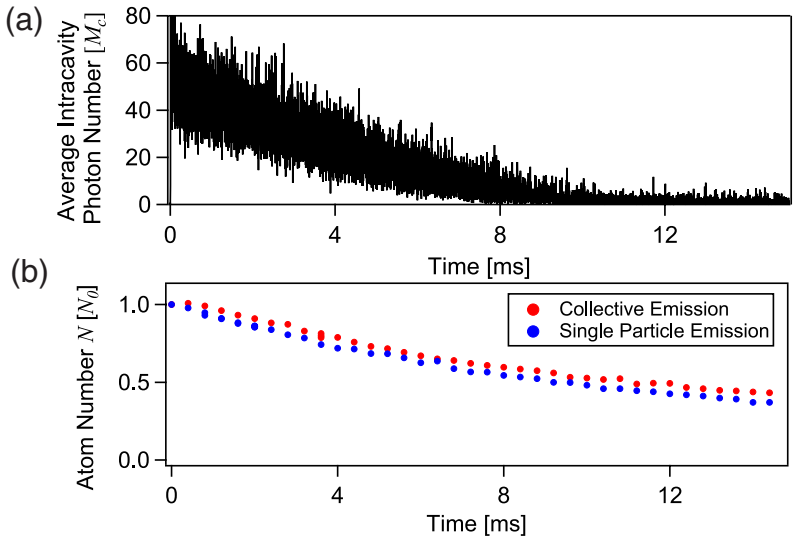

Figure 4. The laser can operate in a quasi-steady-state mode in that each atom can go through an emission-repumping cycle multiple times. However, the emitted power decreases over time, eventually going to zero. In (a), we show one example of emission lasting ~ 10 ms. Under other conditions, we have observed emission lasting up to 120 ms. We verify that atoms are being lost from the trap (b) by measuring a changing frequency shift of the cavity mode consistent with atom loss. The loss is not associated with collective emission, as shown by the equivalence of the loss observed with (red) collective emission or (blue) induced single particle emission from $|e\rangle$ to $|g\rangle$ via free space scattering at the same rate as the collectively enhanced decay rate. The atom number is in units of the initial atom number N_0.

by the atoms. The non-destructive probing is similar to the probing used in spin squeezing experiments [5, 34].

The measured cavity shift decreases the longer the laser is allowed to oscillate, indicating that either atoms are being lost from the trap or are having their coupling to the cavity mode reduced. We verify that atoms are actually being lost from the trap by also performing fluorescence measurements in the same experiment. The decay of the fluorescence signal is consistent with loss of atoms from the trap. The loss of atoms is shown in Fig. 4(b).

The lasing quenches after only half the atoms are lost. This is explained by the fact that the fixed repumping rate W was initially tuned to an optimum value $W \approx N_0 C\gamma_{eg}/2$ for the initial N_0 atoms in the trap. The maximum repumping rate $W_{max} = NC\gamma_{eg}$, above which lasing is quenched as discussed in Sec. 5 below, then crosses below the fixed repumping rate W when the changing atom number N meets the condition $N < N_0/2$.

Lastly, in Fig. 4(b), we present data showing that the loss of atoms is not enhanced by the superradiant process itself. To observe the loss of atoms without superradiant emission, we tune the dressing laser closer to atomic resonance to increase the single particle scattering to $|g\rangle$ to a rate comparable to the collectively enhanced rate. We also move the cavity resonance frequency far from the atomic transition frequency to inhibit any collective enhancement of the decay. After running this non-collective emission for a variable time, we measured the atom number (Fig. 4(b), blue circles). The atom loss was the same as in the case with collective emission (Fig. 4(b), red circles). Because we observe loss from the trap that is not connected to collective emission, we suspect that light assisted collisions, either from the dressing laser or the repumping lasers, are responsible for the atom loss and ultimately for the shutoff of the laser. Light-assisted collisions could be eliminated in the future using higher dimensional trapping lattices.

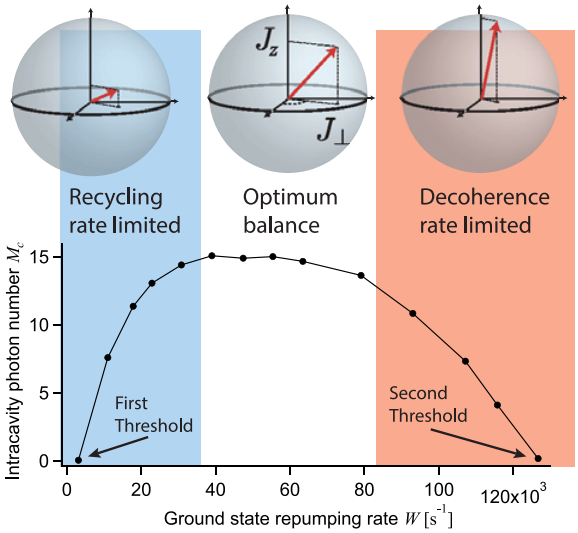

Figure 5. The second laser threshold caused by repumping-induced decoherence as shown by a plot of intracavity photon number (proportional to output power) versus the ground state repumping rate W. To operate with steady-state collective emission, the rate of recycling atoms from the ground state to the excited state must be fast enough to match the single-particle, collectively-enhanced emission rate $\propto NC\gamma_{eg}$. However, the repumping also adds to the decoherence of the atoms, which at high repumping rates can limit the emission rate. The Bloch spheres illustrate the predicted atomic state representing the three regions defined by the blue, white, and red regions.

5. LASER QUENCHING BY REPUMPING-INDUCED DECOHERENCE

In a superradiant laser, one of the dominant sources of decoherence can be the repumping process itself. While a minimum repumping rate is necessary to meet the threshold condition for lasing, the additional decoherence at high repumping rates leads to a second repumping threshold at W_{max} for turn-off in superradiant lasers. We experimentally observe this second threshold as shown in Fig. 5. At low repumping rates, the output power of the laser is just limited by the rate at which the repumping can recycle atoms from the ground state to the excited state, maintaining inversion. Thus, the $\hat{z}$ projection of the Bloch vector J_z and perpendicular projection $J_\perp$ are both small. Under these conditions, the laser output power increases with increasing repumping rate.

At high repumping rates, the repumping destroys the atomic coherence more quickly than the superradiant emission can restore it, leading to a reduction in the $J_\perp$ projection of the Bloch vector, and thus the emitted output power, even though the atomic inversion is large. The collective emission is extinguished when the repumping rate is $W \geq W_{max} = NC\gamma_{eg}$, assuming that the repumping is the dominant decoherence rate in the system. Under the same assumption, the optimum output power is achieved at half the maximum repumping rate $W_{opt} = NC\gamma_{eg}/2$. We have observed this repumping induced turn-off threshold in a superradiant Raman laser, confirming the scaling of the optimum output power and second threshold by studying the repumping threshold for differing induced decay rates γ_{eg} [14].

6. CAVITY PULLING

In general, a laser's emission frequency is a weighted average of the cavity frequency and the optical atomic transition frequency, with relative weights set by the rates κ and $\gamma_\perp$. Deep in the superrradiant

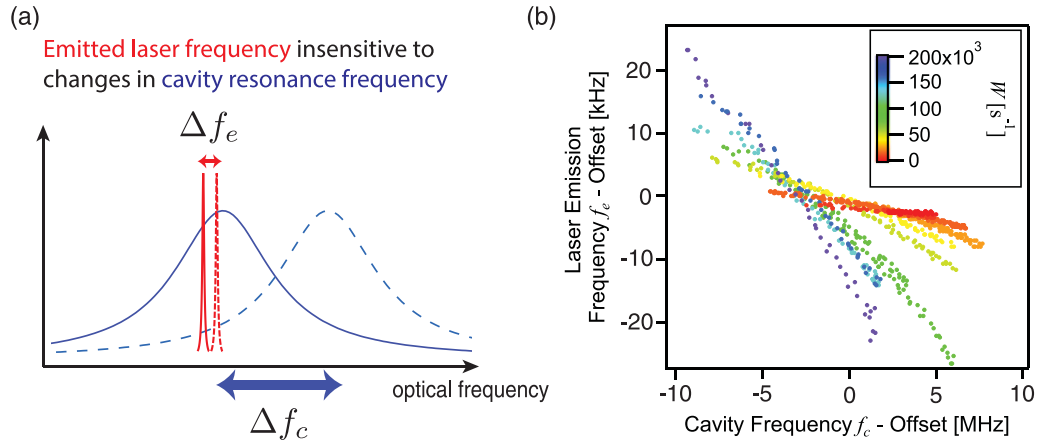

Figure 6. The superradiant laser emission frequency is determined primarily by atomic properties, with a predicted cavity frequency pulling coefficient $P = \gamma_\perp/\kappa$. To measure the cavity pulling, we change the cavity resonance frequency by Δf_c, shown by the shift of broad blue Lorentzian in (a), and then measure the change in the emitted light frequency Δf_e, the shift of the narrow red Lorentzian in (a). The frequencies after the change are represented by the dashed lines. In (b), we show the measured f_e versus f_c for different values of γ_{eg}. The pulling is then $P_{meas} = \Delta f_e/\Delta f_c$, the slope of the data. The repumping rate W is held to $NC\gamma_{eg}/2$, so the pulling coefficient decreases with decreasing γ_{eg}, as seen by the decreasing slopes.

limit, the contribution of the cavity frequency can be expressed as a small pulling of the emission frequency away from the atomic transition frequency and toward the cavity frequency by an amount proportional to the difference between the the emission frequency and the cavity frequency. The frequency pulling coefficient is $P = 2\gamma_\perp/\kappa \approx W/\kappa \ll 1$. This means that the emission frequency of a superradiant laser can be highly immune to noise imposed by a fluctuating cavity resonance frequency.

We observe this suppression of cavity frequency pulling in our superradiant Raman laser. We systematically change the cavity resonance frequency (by changing the cavity length) and observe the laser emission frequency as shown in Fig. 6. For a good-cavity laser, the change in the emission frequency would be equal to the change in the cavity frequency, with a pulling coefficient of $P = 1$. For our superradiant Raman laser, we observe a pulling of the emission frequency with $P = 2 \times 10^{-3}$ to $P = 5 \times 10^{-5}$. The scaling of P with the repumping rate W is shown in Fig. 6. The excited state scattering rate γ_{eg} was also scaled to keep the laser at the optimum repumping rate. As the laser is operated with lower repumping rates, putting it further into the bad-cavity regime, the pulling linearly decreases. This observation of greatly suppressed cavity pulling confirms this key prediction for superradiant lasers.

7. CONCLUSION

In conclusion, we have summarized recent studies of a superradiant Raman laser using laser-cooled ^{87}Rb atoms as the gain medium. The small Doppler broadening enabled by laser cooling and trapping were key to realizing operation deep into the bad-cavity regime $\kappa/\gamma_\perp > 10^4$. The Raman laser functions as a relevant model for proposed ultra-narrow superradiant light sources. The laser can operate quasi-continuously, mapping a collective atomic phase onto the phase of the cavity field. The length of steady-state operation is limited by loss of atoms from the trap. We have confirmed other key predictions for superradiant lasers, including coherent operation with an intracavity field of less than one photon on average, the scaling of the second repumping threshold, and suppression of cavity pulling. We have also studied the amplitude stability of the laser by examining the atomic response using non-demolition

measurements and observed the impact of cavity-feedback for increasing or decreasing the amplitude stability of the laser [15]. Future work will investigate the quantum-limited linewidth of the laser and further explore the spontaneous synchronization responsible for the robust collective coherence.

We thank J. Ye and A.M. Rey for helpful discussions. The authors acknowledge support from NSF PFC, NIST, ARO, DARPA QuASAR, and NSF. J.G. Bohnet acknowledges support from NSF GRF, Z. Chen acknowledges support from A*STAR Singapore, and K.C. Cox acknowledge support from the DoD NSDEG Fellowship Program.

References

[1] K.E. Strecker, G.B. Partridge, A.G. Truscott, R.G. Hulet, Nature **417**, 150 (2002).
[2] J. Appel, P. Windpassinger, D. Oblak, U. Hoff, N. Kjærgaard, E. Polzik, Proc. Natl. Acad. Sci. **106**, 10960 (2009).
[3] C. Deutsch, F. Ramirez-Martinez, C. Lacroûte, F. Reinhard, T. Schneider, J. N. Fuchs, F. Piéchon, F. Laloë, J. Reichel, P. Rosenbusch, Phys. Rev. Lett. **105**, 020401 (2010).
[4] I. D. Leroux, M. H. Schleier-Smith, V. Vuletić, Phys. Rev. Lett. **104**, 073602 (2010).
[5] Z. Chen, J. G. Bohnet, S. R. Sankar, J. Dai, J. K. Thompson, Phys. Rev. Lett. **106**, 133601 (2011).
[6] C. D. Hamley, C. S. Gerving, T. M. Hoang, E. M. Bookjans, M. S. Chapman, Nature Phys. **8**, 305 (2012).
[7] D. Meiser, J. Ye, D. R. Carlson, M. J. Holland, Phys. Rev. Lett. **102**, 163601 (2009).
[8] J. Chen, Chinese Science Bulletin **54**, 348 (2009).
[9] D. Meiser, M. J. Holland, Phys. Rev. A **81**, 033847 (2010).
[10] D. Meiser, M. J. Holland, Phys. Rev. A **81**, 063827 (2010).
[11] M. I. Kolobov, L. Davidovich, E. Giacobino, C. Fabre, Phys. Rev. A **47**, 1431 (1993).
[12] S. J. M. Kuppens, M. P. van Exter, J. P. Woerdman, Phys. Rev. Lett. **72**, 3815 (1994).
[13] H. M. Goldenberg, D. Kleppner, N. F. Ramsey, Phys. Rev. Lett. **5**, 361 (1960).
[14] J. G. Bohnet, Z. Chen, J. M. Weiner, D. Meiser, M. J. Holland, J. K. Thompson, Nature **484**, 78 (2012).
[15] J. G. Bohnet, Z. Chen, J. W. Weiner, K. C. Cox, J. K. Thompson, (to be published in Phys. Rev. Lett.) arXiv:1209.0774[physics.optics].
[16] J. G. Bohnet, Z. Chen, J. W. Weiner, K. C. Cox, J. K. Thompson, arXiv:1208.1710[physics.atom-ph].
[17] J. W. Weiner, K. C. Cox, J. G. Bohnet, Z. Chen, J. K. Thompson, (to be published in Appl. Phys. Lett.) arXiv:1210.3663 [physics.atom-ph].
[18] D. R. Leibrandt, M. J. Thorpe, J. C. Bergquist, T. Rosenband, Opt. Express **19**, 10278 (2011).
[19] G. Vrijsen, O. Hosten, J. Lee, S. Bernon, M. A. Kasevich, Phys. Rev. Lett. **107**, 063904 (2011).
[20] G. Björk, H. Heitmann, Y. Yamamoto, Phys. Rev. A **47**, 4451 (1993).
[21] L. Casperson, IEEE J. Quantum Electron. **14**, 756 (1978).
[22] R. G. Harrison, D. J. Biswas, Phys. Rev. Lett. **55**, 63 (1985).
[23] C. O. Weiss, J. Brock, Phys. Rev. Lett. **57**, 2804 (1986).
[24] A. L. Schawlow, C. H. Townes, Phys. Rev. **112**, 1940 (1958).
[25] T. Kessler, C. Hagemann, C. Grebing, T. Legero, U. Sterr, F. Riehle, M. Martin, L. Chen, J. Ye, Nature Photon. (2012).
[26] L. Hilico, C. Fabre, E. Giacobino, Europhys. Lett. **18**, 685 (1992).
[27] W. Guerin, F. Michaud, R. Kaiser, Phys. Rev. Lett. **101**, 093002 (2008).
[28] H. W. Chan, A. T. Black, V. Vuletić, Phys. Rev. Lett. **90**, 063003 (2003).
[29] J. G. Bohnet, Z. Chen, J. W. Weiner, K. C. Cox, J. K. Thompson, (in preparation).

[30] H. Tanji-Suzuki, I. D. Leroux, M. H. Schleier-Smith, M. Cetina, A. T. Grier, J. Simon, V. Vuletić, in *Advances in Atomic, Molecular, and Optical Physics*, edited by P. B. E. Arimondo, C. Lin (Academic Press, 2011), Vol. 60 of *Advances In Atomic, Molecular, and Optical Physics*, pp. 201–237.
[31] R. H. Dicke, Phys. Rev. **93**, 99 (1954).
[32] R. P. Feynman, F. L. Vernon, R. W. Hellwarth, J. Appl. Phys. **28**, 49 (1957).
[33] M. Gross, S. Haroche, Phys. Rep. **93**, 301 (1982).
[34] H. Zhang, R. McConnell, S. Ćuk, Q. Lin, M. H. Schleier-Smith, I. D. Leroux, V. Vuletić, Phys. Rev. Lett. **109**, 133603 (2012).